NASA Technical Paper 3169

Diffracted and Head Waves Associated With Waves on Nonseparable Surfaces

Raymond L. Barger

March 1992

Abstract

A theory is presented for computing waves radiated from waves on a smooth surface. With the assumption that attenuation of the surface wave is due only to radiation and not to dissipation in the surface material, the radiation coefficient is derived in terms of the attenuation factor. The excitation coefficient is determined by the reciprocity condition. Formulas for the shape and the spreading of the radiated wave are derived, and some sample calculations are presented. An investigation of resonant phase matching for nonseparable surfaces is presented with a sample calculation. A discussion of how such calculations might be related to resonant frequencies of nonseparable thin shell structures is included. A description is given of nonseparable surfaces that can be modeled in the vector form that facilitates use of the appropriate formulas of differential geometry.

1. Introduction

Calculations of surface waves and of waves radiated from surfaces have potential applications in such areas as sound diffraction and shock diffraction by an aerodynamic surface, nondestructive testing (crack detection), mutual coupling of surface-mounted antennas, underwater signal recognition, and resonance of thin shell structures. The geometric theory of diffraction (GTD) developed by J. B. Keller and his associates (ref. 1) three decades ago led to many such applications and to theories for diffraction by a smooth body (ref. 2) and for surface waves on a curved surface (ref. 3). This development, applicable as a high frequency approximation, represented a significant breakthrough in the wave theory involving surfaces for which the wave equation is not separable. By the GTD method, the surface waves could be calculated by ray tracing techniques; then related to waves in the surrounding medium by means of coefficients, variously termed diffraction, excitation, radiation, or launching coefficients. These coefficients could be determined by exact solutions to canonical problems, that is, tractable problems involving separable surfaces. Thus, a large class of smooth surfaces became amenable to surface wave analysis.

However, the results, in terms of actual use, have been disappointing. A cursory survey of the literature yields few, if any, actual GTD calculations involving nonseparable surfaces. Reference 4 describes in detail a procedure for calculating ray paths and wave fronts on such a surface. The purpose of this paper is to supplement reference 4 by relating the surface waves to (1) the diffracted waves or head waves radiated into the surrounding medium, and (2) natural resonance phenomena of thin shell structures. Equations for the radiated waves are derived, and sample calculations illustrate the procedure. (Head waves are waves radiated at an angle not equal to 0°.)

Rays that traverse the surface along a closed path give rise to a resonance effect at critical frequencies (ref. 5). This effect is observed in the diffracted or head wave radiated from the surface. A method for locating closed paths associated with this kind of resonance is described, and an illustrative calculation is included.

2. Symbols

A	amplitude
$\Delta\mathbf{A}$	wave front vector, pointing in direction of wave front normal, with magnitude equal to ray tube cross-sectional area
c_m	wave speed in medium surrounding surface
c_s	surface wave speed
E, F, G	metric coefficients
E_r, G_r	metric coefficients along and normal to surface ray
ΔE	energy flux
e, f, g	coefficients of second fundamental form (curvature coefficients)
$\widehat{I}$	incident ray direction
$\mathbf{I}_{\parallel}$	vector projection of $\widehat{I}$ onto tangent plane
$\hat{\imath}, \hat{\jmath}, \hat{k}$	orthonormal base vector in direction of x, y, and z axis, respectively

K	total (Gaussian) curvature
k	wave number
$\widetilde{m}$	number of times surface ray traverses a caustic
$\widehat{N}$	unit surface normal vector
n	surface distance normal to ray direction
$\hat{p}$	unit vector defined by equation (32)
$\hat{q}$	unit vector normal to $\hat{p}$ in $\widehat{T}, \widehat{N}$ plane
R	radiation coefficient
$\mathbf{r}(u,v)$	vector location of generic surface point
s	distance along ray in surrounding medium
s_P	distance along ray from surface to point P
s_Q	distance along ray from point P to surface
$\widehat{T}$	unit tangent vector to surface ray
t	time on surface ray
t^*	time on ray emitted from surface
u, v	surface coordinates
$\hat{u}$	unit vector normal to $\hat{p}$ and $\hat{q}$
x, y, z	Cartesian coordinates
$\mathbf{x}$	vector location of point on surface ray
$\mathbf{y}$	vector location of point on ray emitted from surface
$\tilde{y}, \tilde{z}$	coordinates of points defining normalized cross-section shape
ε	excitation coefficient
η	parameter distinguishing individual rays emitted from surface at time t
θ	angle of incidence or radiation
$\kappa_{g,n}$	geodesic curvature of surface wave front
$\kappa_{n,n}$	normal curvature of surface wave front in direction $\hat{p}$
κ_p	curvature of surface wave front in direction $\hat{p}$
κ_r	curvature of surface ray
λ	parameter defining a local direction on surface (see eq. (17))
μ	attenuation factor
$\mu(x)$	homotopy function
$\nu(x)$	scaling, or sizing, function
ρ	density
σ	distance along ray path
$d\tau$	cross-sectional area of ray tube
Υ	torsion of surface ray
ϕ	phase
ω	frequency, radians
Subscripts:	
i	initial
f	final
m	condition in surrounding medium
o	initial point of surface ray
P, Q, P_r, Q_i	quantity evaluated at this location
r	surface ray
s	surface

3. General Considerations

First, section 4.1 describes the basic assumptions and scope of the theory. Then section 4.2 demonstrates how a general class of smooth surfaces can be modeled in an appropriate analytic form for the application of the theory and procedures described in the subsequent sections. This section is a brief summary of the method of reference 6. Section 4.3 discusses calculation of surface waves and how they are related to waves in the surrounding medium. Section 4.4 is a discussion of related problems. The strengths of the radiated waves as well as the global representation of their shapes are treated in section 4.5. Several sample calculations of these wave shapes are included in section 5. Section 6 discusses the theory and calculation procedure for finding the closed surface ray paths that give rise to resonance effects.

4. Analysis

4.1. Scope of Theory

Throughout the analysis, the emphasis is placed on theory and methods for determining the geometric quantities that are required for computing wave fields that are emitted by waves on a smooth surface. The

primary assumptions and limitations of the theory are (1) scalar waves, (2) real rays and surfaces, (3) homogeneous surfaces, (4) surrounding medium can support a wave, and (5) radiated rays do not intersect surface rays. An attempt has been made to minimize the complications associated with the specialized physics associated with different types of waves. For example, the discussion is confined to scalar waves. However, in much of the literature on vector waves (ref. 7, for example) the results are synthesized from combinations of results for scalar waves. A brief discussion is included in section 4.4 on some additions and modifications that are required for some particular applications.

The elegant concept of complex rays, utilized in reference 3, is not used in this analysis. Although mathematically efficient, such concepts tend to intimidate many engineers. Only real rays, real surfaces, and real frequencies are treated, with damping due to radiation considered as attenuation and not as an imaginary part of the phase.

Derivations of surface wave speeds have been given in a multitude of papers (ref. 8 and its references) and is not duplicated here. It is assumed that the surface wave speed is known and that it is constant (the surface is homogeneous). It should not be too difficult to extend the analysis and methods to inhomogeneous surfaces inasmuch as a procedure for calculating surface ray paths on such surfaces has already been described (ref. 4). However, the analysis is considerably shortened and simplified by restricting it to homogeneous surfaces for which the ray paths are geodesics.

The surface is assumed to be immersed in a medium that will support a wave whose speed is equal to or less than that of the surface wave speed.

Finally, assumptions concerning the convexity of the surface need to be considered. The usual restriction is to smooth convex surfaces. Requiring smoothness avoids the problems associated with the specialized treatments required for diffraction effects resulting from discontinuities in slope or curvature. Requiring convexity avoids the complications that arise when the surface waves exist simultaneously with incident waves, either from the off-surface source (fig. 1(a)) or from previously diffracted waves from the surface itself if it is inflected (fig. 1(b)). However, a global requirement of convexity is often too severe a restriction. The only restriction required in order to secure the desired simplification is that, for any ray under consideration, the normal curvature must be positive outward over that part of the ray path that is being investigated. For example, if the object is illuminated from a far-field source so that the incident rays all have essentially the same direction, and if the grazing rays diffract along paths that satisfy this requirement, then no difficulties occur if the surface is concave in the direction orthogonal to the surface rays (top part of fig. 2). As a second example, the problem of mutual coupling of surface-mounted antennas depends only on the geodesic ray path connecting the two antennas. Consequently, this problem can be treated if the ray path lies along a convex part of the surface. As a final example, if one is considering the head waves excited by surface waves which move at a speed several times greater than the wave speed in the surrounding medium (as is usually the case) then the requirement for convexity, even in the ray direction, can be relaxed except in the most severe cases. For these waves, the rays are radiated from the surface at such a large angle that they are not likely to strike another part of the surface (bottom part of fig. 2).

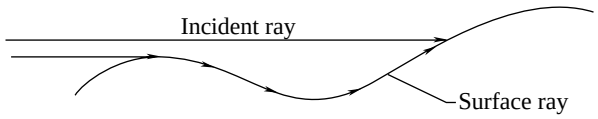

(a) Interaction with incident rays.

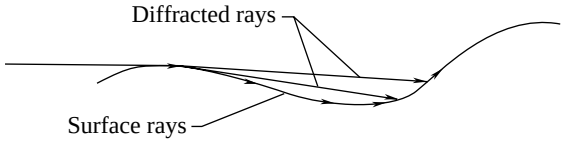

(b) Interaction with diffracted rays.

Figure 1. Interaction of surface rays with incident or diffracted rays on inflected surface.

4.2. Analytically Lofted Surfaces

As was stated in section 1, the analysis and procedures to be described are applicable to a general class of smooth surfaces and are not restricted to

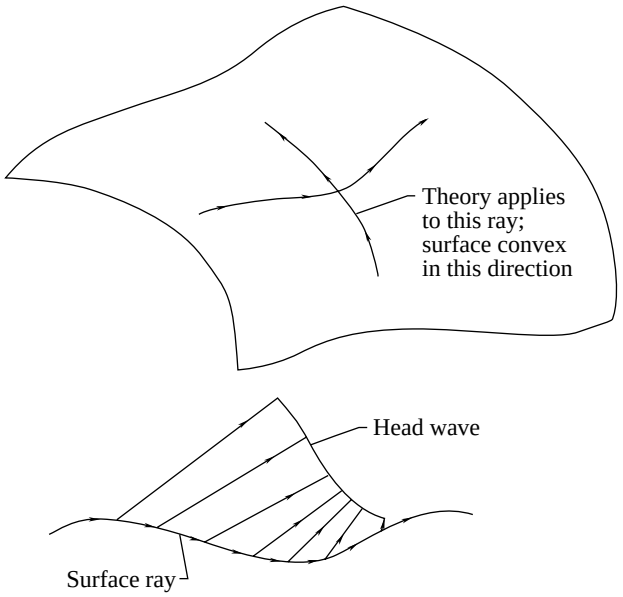

Figure 2. Problems for which theory is applicable on inflected surfaces.

surfaces for which the wave equation is separable. The analysis assumes only that the surface can be expressed as a vector function $\mathbf{r}$ of two variables:

$$\mathbf{r} = \mathbf{r}(u, v) \tag{1}$$

A class of such surfaces, introduced in reference 6 for the purpose of expediting design of aerodynamic components, is described here. These surfaces are defined by specifying the shape of an initial cross section in a plane $x = x_i$ and a final, or terminating, shape at $x = x_f$ and then requiring the intermediate cross sections to represent a smooth transition from the initial to the final shape. The shapes $(y(\xi), z(\xi))$ of the two extreme cross sections are described parametrically in terms of an arbitrary parameter. This parameter might be, for example, the normalized y coordinate, the normalized arc length, the angle in polar coordinates, or the ellipse angle parameter.

Let $\mu(x)$ be a function, varying smoothly and monotonically from 0 to 1 as x varies from x_i to x_f (a homotopy function). Then, for $x_i \le x \le x_f$, a cross-section shape is defined by

$$\tilde{y}(x, \xi) = [1 - \mu(x)]\ y_i(\xi) + \mu(x)\ y_f(\xi) \tag{2a}$$

$$\tilde{z}(x, \xi) = [1 - \mu(x)]\ z_i(\xi) + \mu(x)\ z_f(\xi) \tag{2b}$$

These shapes vary smoothly from the initial shape at $x = x_i$ to the terminating shape at $x = x_f$. By taking ξ as a normalized coordinate, the size variation of the cross sections can be specified by prescribing a scaling function $\nu(x)$, which varies smoothly but not necessarily monotonically from an initial to a final value as x varies from $x = x_i$ to $x = x_f$. The scaled variables are defined by

$$y(x, \xi) = \nu(x)\ \tilde{y}(x, \xi) \tag{3a}$$

$$z(x, \xi) = \nu(x)\ \tilde{z}(x, \xi) \tag{3b}$$

The vector equation of this transition surface is

$$\mathbf{r} = x\hat{\imath} + y(x, \xi)\hat{\jmath} + z(x, \xi)\hat{k} \tag{4}$$

which has the required form (eq. (1)) where the surface variables (u, v) are (x, ξ). For modeling complicated shapes, ν may be allowed to vary with ξ as well as with x, or one may take different scaling functions (ν_y, ν_z) for the (y, z) coordinates. However, for illustrative purposes, equations (3) describe a sufficiently general class of surfaces. The x = Constant lines describe the cross-section shapes, and the ξ = Constant shapes describe the lofting lines. The first derivatives are

$$\mathbf{r}_x = \hat{\imath} + \left[\frac{d\nu}{dx}\ \tilde{y} + \nu\ \frac{d\mu}{dx}\ (y_f - y_i)\right]\hat{\jmath} + \left[\frac{d\nu}{dx}\ \tilde{z} + \nu\ \frac{d\mu}{dx}\ (z_f - z_i)\right]\hat{k} \tag{5a}$$

$$\mathbf{r}_\xi = \nu\left[(1-\mu)\ \frac{dy_i}{d\xi} + \mu\ \frac{dy_f}{d\xi}\right]\hat{\jmath} + \nu\left[(1-\mu)\ \frac{dz_i}{d\xi} + \mu\ \frac{dz_f}{d\xi}\right]\hat{k} \tag{5b}$$

The second derivatives are

$$\mathbf{r}_{xx} = \left[\frac{d^2\nu}{dx^2}\ \tilde{y} + 2\ \frac{d\nu}{dx}\frac{d\mu}{dx}\ (y_f - y_i) + \nu\ \frac{d^2\mu}{dx^2}\ (y_f - y_i)\right]\hat{\jmath} + \left[\frac{d^2\nu}{dx^2}\ \tilde{z} + 2\ \frac{d\nu}{dx}\frac{d\mu}{dx}\ (z_f - z_i) + \nu\ \frac{d^2\mu}{dx^2}\ (z_f - z_i)\right]\hat{k} \tag{6a}$$

$$\mathbf{r}_{x\xi} = \frac{d\nu}{dx}\left[(1-\mu)\ \frac{dy_i}{d\xi} + \mu\ \frac{dy_f}{d\xi} + \nu\ \frac{d\mu}{dx}\left(\frac{dy_f}{d\xi} - \frac{dy_i}{d\xi}\right)\right]\hat{\jmath} + \frac{d\nu}{d\xi}\left[(1-\mu)\ \frac{dz_i}{d\xi} + \mu\ \frac{dz_f}{d\xi} + \nu\ \frac{d\mu}{dx}\left(\frac{dz_f}{d\xi} - \frac{dz_i}{d\xi}\right)\right]\hat{k} \tag{6b}$$

$$\mathbf{r}_{\xi\xi} = \nu\left[(1-\mu)\ \frac{d^2y_i}{d\xi^2} + \mu\ \frac{d^2y_f}{d\xi^2}\right]\hat{\jmath} + \nu\left[(1-\mu)\ \frac{d^2z_i}{d\xi^2} + \mu\ \frac{d^2z_f}{d\xi^2}\right]\hat{k} \tag{6c}$$

With equations (4) through (6) all the geometric parameters required for the surface wave calculations can be computed.

4.3. Ray Tubes and Ray Strips

The surface wave speed is assumed to be constant. Consequently the ray paths, which by Fermat's principle are least time paths, will also be paths of minimum distance, or geodesic lines. Given a point on the surface and an initial direction, a geodesic having these initial conditions can be calculated by a marching procedure. (See ref. 4 for details.)

For the purpose of analyzing the surface rays, two surface coordinate systems are utilized. One is the natural (u, v) coordinate system that is used to define the surface itself. For this system, the metric coefficients are

$$E = \mathbf{r}_u \cdot \mathbf{r}_u \tag{7a}$$

$$F = \mathbf{r}_u \cdot \mathbf{r}_v \tag{7b}$$

$$G = \mathbf{r}_v \cdot \mathbf{r}_v \tag{7c}$$

and the discriminant is

$$H = \sqrt{EG - F^2} \tag{8}$$

The local surface normal is

$$\widehat{N} = \frac{\mathbf{r}_u \times \mathbf{r}_v}{H} \tag{9}$$

and the curvature coefficients, or coefficients of the second fundamental form, are

$$e = \mathbf{r}_{uu} \cdot \widehat{N} \tag{10a}$$

$$f = \mathbf{r}_{uv} \cdot \widehat{N} \tag{10b}$$

$$g = \mathbf{r}_{vv} \cdot \widehat{N} \tag{10c}$$

where the notation is consistent with that of reference 9.

The second coordinate system used consists of time t along a family of rays all initiated at a given time t_o and a surface coordinate normal to the rays (fig. 3). Thus, incremental distance along the rays is

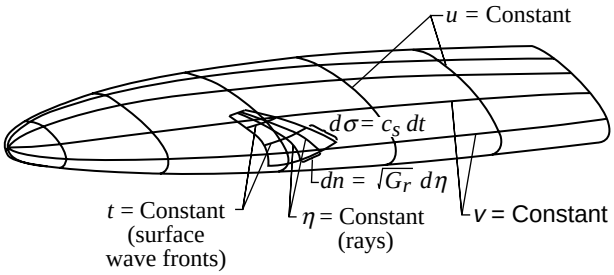

Figure 3. Basic geometry illustrating surface parameters u, v, t, and η.

$$d\sigma = \sqrt{E_r} = c_s \, dt \tag{11}$$

The incremental arc length normal to the rays (that is, along the surface wave fronts) is

$$dn = \sqrt{G_r} \, d\eta \tag{12}$$

where G_r is to be determined and $d\eta$ is the arbitrary increment that distinguishes two adjacent rays. It can be taken as the distance between the rays along the initial excitation line. The metric coefficient G_r is determined as follows. As each point (u_r, v_r) is computed, the local values of e, f, g, and H are computed. From these, the local value of the Gaussian curvature K is calculated by the formula

$$K = \frac{eg - f^2}{H^2} \tag{13}$$

Then G_r is computed by numerical integration of the equation

$$\frac{d^2\sqrt{G_r}}{dt^2} + c_s^2 K \sqrt{G_r} = 0 \tag{14}$$

(The factor c_s^2 was inadvertently omitted in equations (25) and (29) of ref. 4.) The geodesic curvature of the surface wave front is also needed. It is obtained from G_r by the formula

$$\kappa_{g,n} = \frac{1}{\sqrt{G_r}} \frac{d\sqrt{G_r}}{d\sigma} = \frac{1}{c_s\sqrt{G_r}} \frac{d\sqrt{G_r}}{dt} \tag{15}$$

The geodesic curvature of the ray itself is zero by definition. The local surface normal curvature $\kappa_{n,r}$ in the direction of the ray is

$$\kappa_{n,r} = \frac{e + 2f\lambda + g\lambda^2}{E + 2F\lambda + G\lambda^2} \tag{16}$$

where

$$\lambda = \frac{dv}{du} \tag{17}$$

on the ray. The normal curvature in the direction of the wave front is similarly

$$\kappa_{n,n} = \frac{e + 2f\lambda_n + g\lambda_n^2}{E + 2F\lambda_n + G\lambda_n^2} \tag{18}$$

where λ_n is the direction orthogonal to the rays.

The initial locations and directions for rays excited by an off-surface source are determined as follows. Let $\widehat{I} = I_1\hat{\imath} + I_2\hat{\jmath} + I_3\hat{k}$ denote the direction vector from the source to an arbitrary point (u, v) on the surface. Then at (u, v), the conditions

$$\widehat{I}(u,v) \cdot \widehat{N}(u,v) = \cos\theta \tag{19}$$

where

$$\sin\theta = \frac{c_m}{c_s} \tag{20}$$

must be satisfied. The locus of the initial excitation line is then found by numerical solution of equation (19). In practice, one usually selects values of u or v and solves equation (19) for the remaining variable (e.g., search along a $u =$ Constant line for a value of v that satisfies the equation). For a far-field source, $\widehat{I}$ is constant, and for Franz (creeping) waves initiated by grazing rays, $\cos\theta = 0$.

To determine the initial ray direction λ_o, we take a step $d\mathbf{r}$ from $\mathbf{r}_o$ at (u, v):

$$d\mathbf{r} = (x_u\ du + x_v\ dv)\hat{\imath} + (y_u\ du + y_v\ dv)\hat{\jmath} + (z_u\ du + z_v\ dv)\hat{k} \tag{21}$$

If the surface rays are launched by grazing rays ($\theta = 90°$), $d\mathbf{r}$ must be parallel to $\widehat{I}$. If $\theta < 90°$, $d\mathbf{r}$ must still be parallel to the projection of $\widehat{I}$ onto the tangent plane at $\mathbf{r}_o$. In either case, the components of $d\mathbf{r}$ must be proportional to those of $\mathbf{I}_{\|} \equiv \widehat{I} - (\widehat{I}\cdot\widehat{N})\widehat{N}$. For example,

$$\frac{y_u\ du + y_v\ dv}{x_u\ du + x_v\ dv} = \frac{\mathbf{I}_{\|,2}}{\mathbf{I}_{\|,1}} \tag{22a}$$

$$\frac{y_u + y_v\lambda_o}{x_u + x_v\lambda_o} = \frac{\mathbf{I}_{\|,2}}{\mathbf{I}_{\|,1}} \tag{22b}$$

$$\lambda_o = \frac{y_u - \left(\frac{\mathbf{I}_{\|,2}}{\mathbf{I}_{\|,1}}\right) x_u}{x_v - y_v} \tag{22c}$$

Clearly, any two components of $d\mathbf{r}$ could have been chosen for this calculation.

Let A_s denote the amplitude of the surface wave. Then, following the analysis of reference 2 (eqs. (4) through (6)), we assume that the energy radiated into the medium from an increment $d\sigma$ of a ray strip is proportional to A_s^2 and to the area $d\sigma\ dn$ of the ray strip that radiates this energy. Thus,

$$\rho_s c_s \left[A_s^2(\sigma + d\sigma)\ dn\ (\sigma + d\sigma) - A_s^2(\sigma)\ dn\ d\sigma\right] = \rho_s c_s \left[2\mu(\sigma) A_s^2\ dn\ d\sigma\right] \tag{23}$$

where, again consistent with reference 2, $2\mu(\sigma)$ is taken to be the proportionality constant. The attenuation factor μ is preferably determined by experiment if such data are available, but otherwise, it is determined by solution of the wave equation for a canonical problem. Expressions for μ are tabulated in reference 2 for several types of boundary conditions.

Equation (23) leads to the differential equation

$$\frac{d}{d\sigma}(A_s^2\ dn\ \rho_s c_s) = -2\mu(A_s^2\ dn\ \rho_s c_s) \tag{24a}$$

$$d(A_s^2\ dn\ \rho_s c_s) = -2\mu(A_s^2\ dn\ \rho_s c_s)\ d\sigma \tag{24b}$$

whose solution is

$$A_s(\sigma) = A_{\sigma,o}\left(\frac{dn_o}{dn}\right)^{1/2} \exp\left[-\int_0^\sigma \mu(\sigma)\ d\sigma\right] \tag{25}$$

The phase on the ray strip is

$$\phi = \phi_o + k\sigma \tag{26a}$$

$$\phi = \phi + kc_s t \tag{26b}$$

For the rays radiated from the surface, the GTD theory assumes that the amplitude of the radiated ray is proportional to the amplitude of the surface ray (ref. 3):

$$A_r = RA_s \tag{27}$$

For the radiated ray tube, the energy flux is

$$\Delta E_r = A_r^2\ d\tau\ \rho_m c_m \tag{28}$$

where $d\tau$ is the cross-sectional area of the ray tube. At the surface (fig. 4),

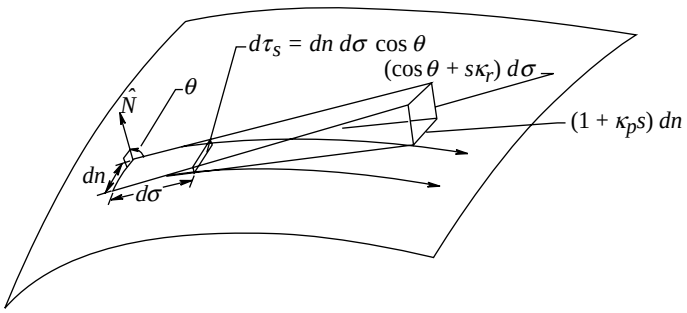

Figure 4. Geometry of ray tube cross-sectional area.

$$d\tau_s = dn\ d\sigma\ \cos\ \theta \tag{29}$$

Equating the expression in equation (28) to the magnitude of the energy flux in equation (24b) and using equations (27) and (29) yield

$$2\mu A_s^2 \rho_s c_s\ d\sigma\ dn = R^2 A_s^2 \rho_m c_m\ dn\ d\sigma\ \cos\ \theta \tag{30}$$

from which

$$R^2 = \frac{2\mu}{\cos\ \theta} \frac{\rho_s c_s}{\rho_m c_m} \tag{31}$$

This method of obtaining the radiation coefficient from the attenuation factor μ could also be applied inversely. That is, if R were determined directly from a solution to a canonical problem, then μ could be obtained from R.

Let $\hat{p}$ denote the direction vector of a radiated ray

$$\hat{p} = \sin\ \theta\ \widehat{T} + \cos\ \theta\ \widehat{N} \tag{32}$$

and let $\hat{q}$ denote the unit vector normal to $\hat{p}$ in the $\widehat{T}, \widehat{N}$ plane. (See fig. 5.) The change in $\hat{p}$ over the distance σ, in the $\widehat{T}, \widehat{N}$ plane, is

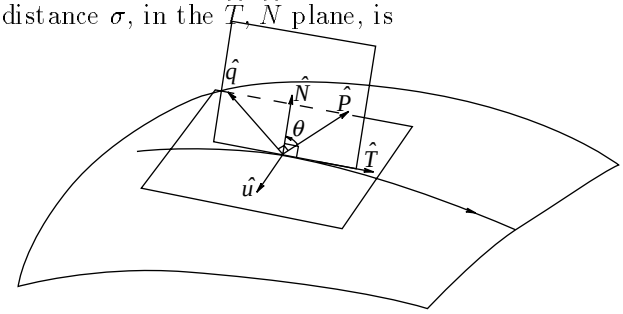

Figure 5. Orientation of unit vectors in tangent $(\widehat{T}, \hat{u})$ plane and in radiation $(\widehat{T}, \widehat{N})$ plane.

$$\left(\hat{q} \cdot \frac{d\hat{p}}{d\sigma}\right)\ d\sigma = \left(\cos\ \theta\ \widehat{T} - \sin\ \theta\ \widehat{N}\right) \cdot \left(\kappa_r \sin\ \theta\ \widehat{N} - \kappa_r\ \cos\ \theta\ \widehat{T}\right)\ d\sigma \tag{33a}$$

$$\left(\hat{q} \cdot \frac{d\hat{p}}{d\sigma}\right)\ d\sigma = \kappa_r\ d\sigma \tag{33b}$$

Let κ_n denote the curvature vector of the surface wave front. The variation of $\hat{p}$ over the distance dn along the surface wave front is

$$(\kappa_n \cdot \hat{p}) = (\kappa_{n,n}\ \cos\ \theta\ +\ \kappa_{n,g}\ \sin\ \theta)\ dn \equiv \kappa_p\ dn \tag{34}$$

The angular increment along the ray over distance $d\sigma$ is given by equation (34), and the angular increment over dn normal to the ray is given by equation (33b). Thus the spreading of rays emitted from this incremental area is $s\kappa_r\ d\sigma$ in the $\widehat{N}, \widehat{T}$ plane, and $s\kappa_p\ dn$ normal to this plane. The actual ray tube area at distance s from the surface, measured along the ray, is obtained by adding these increments to the increments at the surface (eq. (29)), which yields (see fig. 4)

$$d\tau_s = (\cos\ \theta + s\kappa_r)\ d\sigma\ (1 + \kappa_p s)\ dn \tag{35}$$

By formulas (27), (29), and (35), the amplitude A_P at point P is given by

$$\frac{A_r^2}{A_P^2} = \frac{(\cos\ \theta\ d\sigma + \kappa_r s\ d\sigma)(dn + \kappa_p s\ dn)}{d\sigma\ dn\ \cos\ \theta} \tag{36a}$$

$$\frac{A_r^2}{A_P^2} = (\cos\ \theta + \kappa_r s)(1 + \kappa_p s)\ \sec\ \theta \tag{36b}$$

where s is the distance from the radiation point P_r to P. A more general form of equation (35) is given in reference 9.

A problem arises with Franz waves for which $\theta = \frac{\pi}{2}$, since in this case R in equation (31) increases indefinitely. The singular nature of the radiation coefficient and the caustic condition at the surface are discussed at length in the literature (refs. 2 and 3, for example). However, this singular character has a somewhat artificial quality, since it arises from the manner in which the physical phenomena are modeled rather than the actual physical process. If we relate the amplitude at P directly to the surface wave amplitude by equations (27), (31), and (36), we get the nonsingular result

$$\begin{aligned} \frac{A_P^2}{A_s^2} &= \left(\frac{A_P}{A_r}\right)^2 \left(\frac{A_r}{A_s}\right)^2 \\ &= R^2 \frac{\cos\ \theta}{(\cos\ \theta + \kappa_r s_P)(1 + \kappa_p s_P)} \\ &= \frac{2\mu}{(\cos\ \theta + \kappa_r s_P)(1 + \kappa_p s_P)} \frac{\rho_s c_s}{\rho_m c_m} \end{aligned} \tag{37}$$

If the surface wave is excited by an off-surface source at Q (fig. 6), the initial amplitude on the surface at the excitation point Q_i is related to that of the incoming wave by an excitation coefficient ε:

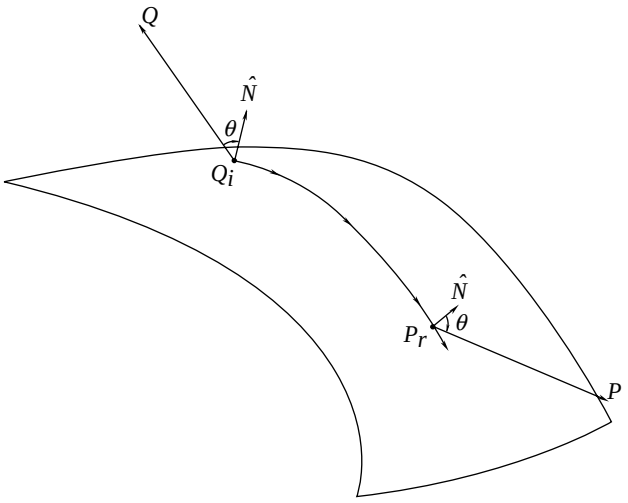

Figure 6. Incident, surface, and radiated rays.

$$A_{s,0} = \varepsilon(Q_i)\, A_i \tag{38}$$

where A_i is related to a source strength $\widetilde{A}$ at Q by

$$A_i^2 = \frac{\widetilde{A}^2}{s_Q} \tag{39}$$

(See fig. 6.) Combining equations (38), (37), (25), and (36) yields

$$A_P^2 = \left(\frac{A_P}{A_s}\right)^2 \left(\frac{A_s}{A_{s,o}}\right)^2 \left(\frac{A_{s,o}}{A_i}\right)^2 \left(\frac{A_i}{\widetilde{A}}\right)^2 \widetilde{A}^2 \tag{40a}$$

$$= \left[\frac{2\mu}{(\cos\ \theta + \kappa_r s_P)(1+\kappa_p s_P)}\right]_{P_r} \left(\frac{dn_o}{dn}\right)$$

$$\times\ \exp\left(-\int_0^\sigma \mu\, d\sigma\right) \frac{\varepsilon(Q_i)}{s_Q}\, \widetilde{A}^2 \tag{40b}$$

where the subscript P_r denotes that the quantity is evaluated at the radiation point P_r.

To determine the excitation coefficient ε_Q, we apply the reciprocity principle, which states that an equal field is obtained at Q if the source is located at P instead of at Q. Since for both cases the surface ray path is the same, the spreading factor dn_o/dn is the same if the directions are reversed on the path. This follows from equations (12) and (14), which demonstrate that the ray strip spreading is determined by the distribution of the Gaussian curvature along the path. Furthermore, the attenuation due to spreading is clearly the same for both the forward and the reverse directions. Consequently, when the forward and reverse amplitudes obtained from equation (40b) are equated, the reciprocity principle yields

$$\frac{\varepsilon_Q}{s_Q\left[(\cos\ \theta + \kappa_r s)(1+\kappa_p s)\right]_{P_r}} = \frac{\varepsilon_P}{s_P\left[(\cos\ \theta + \kappa_r s)(1+\kappa_p s)\right]_{Q_i}} \tag{41}$$

Thus, in order for reciprocity to be satisfied ($\varepsilon_P = \varepsilon_Q$), we must have

$$\varepsilon_Q = \frac{s_Q}{\left[(\cos\ \theta + \kappa_r s)(1+\kappa_p s)\right]_{Q_i}} \tag{42}$$

In this formula, $(\kappa_p)_{Q_i}$ is the component in the direction $-\widehat{I}$ of the curvature vector of the initial wave front, which is found by solving equation (19) numerically, as was discussed earlier. Also, κ_r is the surface curvature in the surface direction λ_o as computed from equations (16) and (22c).

The phase ωt along the ray path is

$$\phi = \omega\left(t_Q + \frac{s_Q}{c_m} + \frac{1}{c_s}\int_{Q_i}^{P_r} d\sigma + \frac{s_P}{c_m}\right) \tag{43}$$

Appropriate phase jumps of integer multiples of $\pi/2$ must be included if the ray traverses caustic points.

4.4. Discussion of Related Problems

In deriving the relationship between the attenuation factor and the radiation coefficient, the attenuation is assumed to be caused only by the radiation of energy from the surface. If the waves penetrate the surface and attenuation also occurs because of dissipation or inhomogeneity, such attenuation must be included in the analysis. Reference 9 considers waves in a ray tube adjacent to the surface and obtains a somewhat different result from that of Levy and Keller (ref. 2) for waves satisfying the impedance boundary condition at the surface. For certain elastic waves, a change in wave type occurs as the wave in the medium excites a surface wave or is emitted from the surface (ref. 10). As might be expected, in this case the factor $\rho_m c_m/\rho_s c_s$ in equation (31) is not unity.

As was mentioned earlier, vector waves are often treated by synthesizing the solutions from those of scalar waves. The polarization of the waves, however, depends on the torsion of the ray path. The torsion may be computed at each point on the path by first

computing $\widehat{N}$ and the quotient $d\widehat{N}/d\sigma$ and using the formula (ref. 11, p. 201)

$$\Upsilon(\sigma) = \widehat{T} \times \widehat{N} \cdot \frac{d\widehat{N}}{d\sigma} \tag{44}$$

Actually, the quantity $d\widehat{N}/d\sigma$ is the crucial factor since, for perfectly conducting surfaces, the wave is polarized normal to the surface.

4.5. Wave Fronts and Strengths

In section 4.3 it was shown that one can compute surface geodesic ray paths and express the location of points on these rays in terms of coordinates t and η, where t is time elapsed from the point of excitation and η distinguishes the individual rays. Now the local wave front surface at an arbitrary time t^* is expressed in the vector form of equation (1) in order to more easily study the surface geometry of the wave front. For this purpose the surface variables u, v in equation (1) are taken to be (t, η). Since c_s is assumed to be constant, we could replace the coordinate t with $\sigma = c_s t$. Denoting a point on a surface ray by $\mathbf{x}(t, \eta)$, the ray emitted from $\mathbf{x}(t, \eta)$ passes at time t^* through the point

$$\mathbf{y}(t, \eta) = \mathbf{x}(t, \eta) + c_m(t^* - t)\ \hat{p}(t, \eta) \tag{45}$$

where $\hat{p}$ is the direction vector defined by equation (32). Utilizing equation (45), which has the required form of equation (1), we can derive an expression for the wave front surface area element and thereby verify formula (35) for the ray tube cross-sectional area.

We denote the direction normal to $\hat{p}$ in the $\widehat{T}, \widehat{N}$ plane by $\hat{q}$ (fig. 5). Then

$$\hat{q}(t, \eta) = \cos\ \theta\ \widehat{T} - \sin\ \theta\ \widehat{N} \tag{46}$$

We can solve equations (32) and (46) for $\widehat{T}$

$$\widehat{T} = \sin\ \theta\, \hat{p} + \cos\ \theta\ \hat{q} \tag{47}$$

We define a unit vector $\hat{u}$ orthogonal to the $\widehat{N}, \widehat{T}$ plane, which is also the $\hat{p}, \hat{q}$ plane. (See fig. 5.) Then $\hat{p}, \hat{q}, \hat{u}$ form an orthonormal set. The derivative of $\mathbf{y}(t, \eta)$ with respect to t is

$$\frac{d\mathbf{y}}{dt} = \frac{d\mathbf{x}}{dt} - c_m\hat{p} + s\ \frac{d\hat{p}}{dt} \tag{48a}$$

This equation can also be written

$$\frac{d\mathbf{y}}{dt} = c_s\widehat{T} - c_m\hat{p} + sc_s\ \frac{d\hat{p}}{d\sigma} \tag{48b}$$

where, from equation (32) and the Frenet formulas,

$$\frac{d\hat{p}}{d\sigma} = \sin\ \theta\ \frac{d\widehat{T}}{d\sigma} + \cos\ \theta\ \frac{d\widehat{N}}{d\sigma} \tag{49a}$$

$$\frac{d\hat{p}}{d\sigma} = \sin\ \theta\ \kappa_r\widehat{N} + \cos\ \theta\ \left(\kappa_r\widehat{T} + \Upsilon_r\hat{u}\right) \tag{49b}$$

$$\frac{d\hat{p}}{d\sigma} = \kappa_r\hat{q} + \cos\ \theta\ \Upsilon_r\hat{u} \tag{49c}$$

where Υ_r is the torsion of the surface ray and $\widehat{N}$ points are in the opposite direction from the curvilinear vector of the geodesic ray path.

Substituting equations (47) and (49c) into (48b) yields

$$\frac{d\mathbf{y}}{dt} = c_s \sin\ \theta\ \hat{p} + c_s\ \cos\ \theta\ \hat{q} - c_m\hat{p} + sc_s\kappa_r\hat{q} + sc_s\ \cos\ \theta\ \Upsilon_r\hat{u} \tag{50a}$$

which, with the assumption of equation (20), becomes

$$\frac{d\mathbf{y}}{dt} = c_s(\cos\ \theta\ + s\kappa_r)\hat{q} + c_s s\ \cos\ \theta\ \Upsilon_r\hat{u} \tag{50b}$$

Differentiating $\mathbf{y}$ with respect to η yields

$$\frac{d\mathbf{y}}{d\eta} = \frac{d\mathbf{x}}{d\eta} + s\ \frac{d\hat{p}}{d\eta} \tag{51}$$

where

$$\frac{d\hat{p}}{d\eta} = \sqrt{G_r}\ \frac{d\hat{p}}{dn} \tag{52a}$$

$$\frac{d\hat{p}}{d\eta} = \sqrt{G_r}\left(\sin\ \theta\ \frac{d\widehat{T}}{dn} + \cos\ \theta\ \frac{d\widehat{N}}{dn}\right) \tag{52b}$$

$$\frac{d\hat{p}}{d\eta} = \sqrt{G_r}\left(\sin\ \theta\ \kappa_{n,g}\hat{u} + \cos\ \theta\ \kappa_{n,n}\hat{u}\right) \tag{52c}$$

$$\frac{d\hat{p}}{d\eta} = \sqrt{G_r}\kappa_p\hat{u} \tag{52d}$$

Thus

$$\frac{d\mathbf{y}}{d\eta} = \sqrt{G_r}(1 + s\kappa_p)\hat{u} \tag{53}$$

The wave front vector is

$$\Delta\mathbf{A} = \left(\frac{d\mathbf{y}}{dt} \times \frac{d\mathbf{y}}{d\eta}\right) d\eta\ dt \tag{54}$$

which yields (with eqs. (11), (12), (50b), and (53))

$$\Delta\mathbf{A} = \begin{vmatrix} \hat{p} & \hat{q} & \hat{u} \\ 0 & c_s(\cos\ \theta + \kappa_r s) & c_s\ \cos\ \theta\ s\ \Upsilon_r \\ 0 & 0 & \sqrt{G_r}(1+s\kappa_p) \end{vmatrix} \frac{d\sigma\ dn}{c_s\sqrt{G_o}} \tag{55a}$$

$$= (1+s\kappa_p)(\cos\ \theta + \kappa_r s)\ dn\ d\sigma\ \hat{p} \tag{55b}$$

Thus $\hat{p}$ is the wave front normal direction, and the ray tube cross-section area is

$$d\tau = (1+s\kappa_p)(\cos\ \theta + \kappa_r s)\ dn\ d\sigma \tag{56}$$

which is consistent with that determined in the previous section (see eq. (35)) and, thus, provides an independent verification of the theory. One could also differentiate equations (50b) and (53) to obtain the curvatures of the wave front surface in terms of those of the radiating surface.

It is of interest to study the wave front equation (eq. (45)) in the limiting two-dimensional case. That is, we consider waves radiated from a cylinder having a smooth cross-section shape which is arbitrary within the constraint that none of the radiated rays are incident on the surface. Then equation (45) becomes

$$\mathbf{y}(t) = \mathbf{x}(t) + c_m(t^* - t)\hat{p}(t) \tag{57}$$

and equation (50b) simplifies to

$$\frac{d\mathbf{y}}{dt} = (c_s\ \cos\ \theta + \kappa_r)\hat{q}(t) \tag{58}$$

In particular, if we treat Franz (creeping) waves initiated by a ray grazing a convex cylinder at a point Q (fig. 7), then, since for this case $c_s = c_m$, the constant phase at the wave front corresponds to a constant distance the rays travel over the surface from Q_i to $\mathbf{x}(t)$ and from $\mathbf{x}(t)$ to $\mathbf{y}$. Consequently,

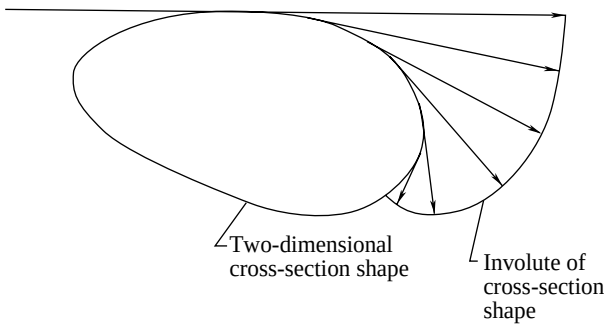

Figure 7. Shape of diffracted wave front emitted by Franz waves.

the diffracted wave front represents the involute of the curve that defines the cross-section shape of the diffracting surface. In this case, equations (57) and (58) become, respectively,

$$\mathbf{y}(t) = \mathbf{x}(t) + c_m(t^* - t)\widehat{T}(t) \tag{59}$$

and

$$\frac{d\mathbf{y}}{dt} = \kappa_r(t)\widehat{N}(t) \tag{60}$$

5. Sample Calculations

In the following examples, the ray calculations were performed by the method of reference 4. The high accuracy of the method was verified by comparing a numerical calculation with the known helical geodesic on a circular cylinder. For the illustrative example shown in figure 8, the surface was defined with the initial cross section taken to be an ellipse having a ratio of minor to major axis of 1/3, and the base section is an ellipse having a ratio of 0.58. This surface is smooth and convex but not separable. Figure 8(a) shows the results of a Franz wave calculation with an illuminating beam having direction numbers (1,7,2). For clarity in presentation, only a portion of the surface wave and the corresponding diffracted wave are shown. Figures 8(b) and (c) show a similar calculation from different viewing angles but with the surface wave speed c_s three times greater than the wave speed c_m in the medium.

6. Resonant Phase Matching

If we compute a geodesic ray path that completely circumnavigates a smooth body, the path may close on itself. That is, it may return to the initial point propagating in the initial direction. This always occurs on spheres and in two-dimensional situations. Furthermore, it occurs for propagation along the maximum or minimum meridian line on a spheroid or any smooth closed surface that has a maximum or minimum meridian.

When such a closed path exists, a resonant condition occurs for a frequency such that the phase accumulation over the closed path is an integer multiple m of 2π. Since surface waves over closed surfaces form caustics, this phase accumulation must include a shift of $\pi/2$ for each time the ray traverses a caustic point. In equation form

$$\frac{\omega}{c_s}\oint ds - \widetilde{m}\ \frac{\pi}{2} = 2\pi m \tag{61}$$

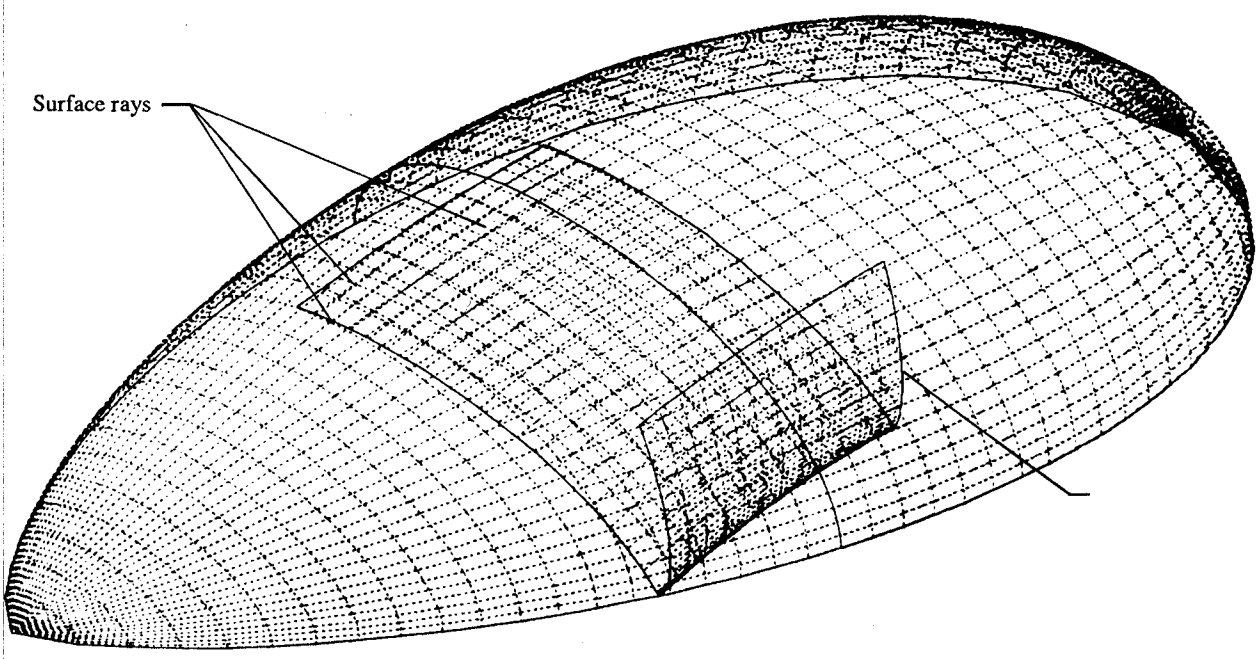

(a) $\theta = 90°$.

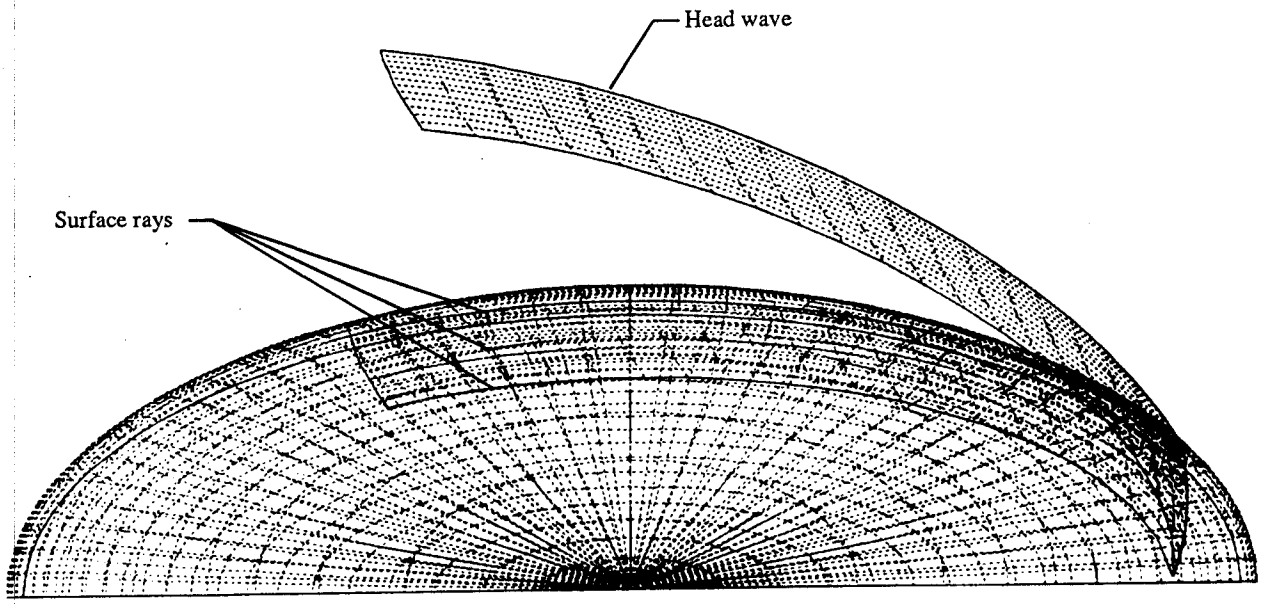

(b) $\theta = \cos^{-1} \frac{1}{3}$; front view.

Figure 8. Surface wave and wave emitted from surface.

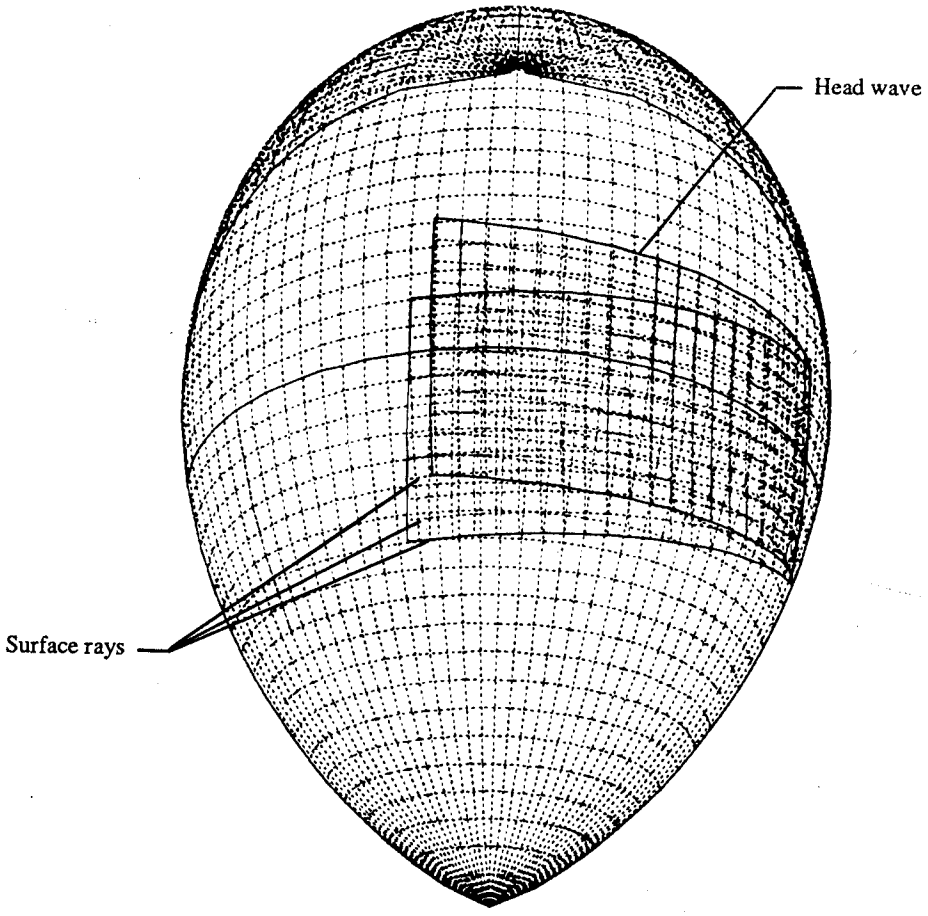

(c) $\theta = \cos^{-1}\frac{1}{3}$; view from above surface.

Figure 8. Concluded.

where $\tilde{m}$ is the number of caustic traversals. The calculation of resonant condition rays for separable surfaces and the relation of the corresponding resonant frequencies of the natural frequencies of the body have been reported by Überall and his associates in several papers (refs. 12 and 13). In order to determine a resonant condition for a nonseparable surface, one must first find a closed surface ray path and then determine the number of times the ray traverses a caustic over this path.

The body used for the surface calculations of figure 8 was investigated to locate closed ray paths. Obvious closed paths exist along the maximum and minimum meridian lines. In addition to these cases, another type of closed path was found (by an iterative procedure), as shown in figure 9. Here, the ray circumnavigates the body twice before the closed circuit is complete. The caustic points on this path are points where G_r vanishes. For illustrative purposes, an adjacent ray was calculated in order to display the ray strip with its two caustics in the closed ray path.

Thus, for this case, if σ_c is the closed path length, resonance occurs for

$$\omega_m = \frac{c_s}{\sigma_c}(2m+1)\pi \tag{62}$$

In this situation, if the wave is a Franz wave, the effect of the resonance is seen in the rays diffracted from the surface along this closed ray path. However, if the surface wave is initiated by a grazing ray from a far-field source, the effect is not observed at the source because no ray is diffracted along this path in the direction of the source. It could be detected by a detector (microphone or antenna) in a bistatic arrangement. This kind of closed ray path might also affect the mutual interference of surface mounted antennas, although the primary concern for

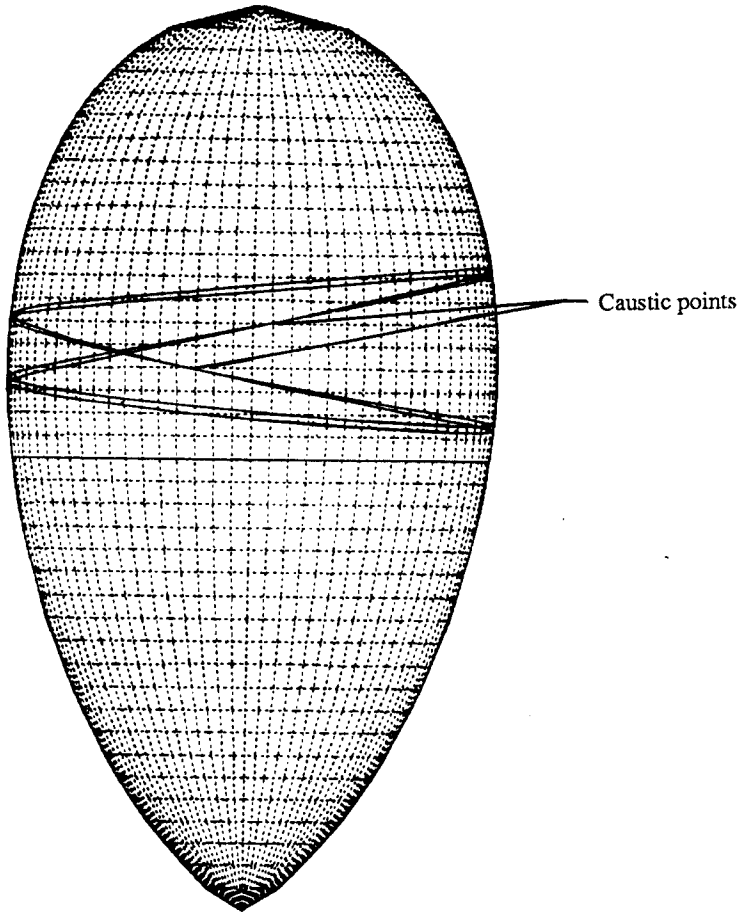

(a) Top view.

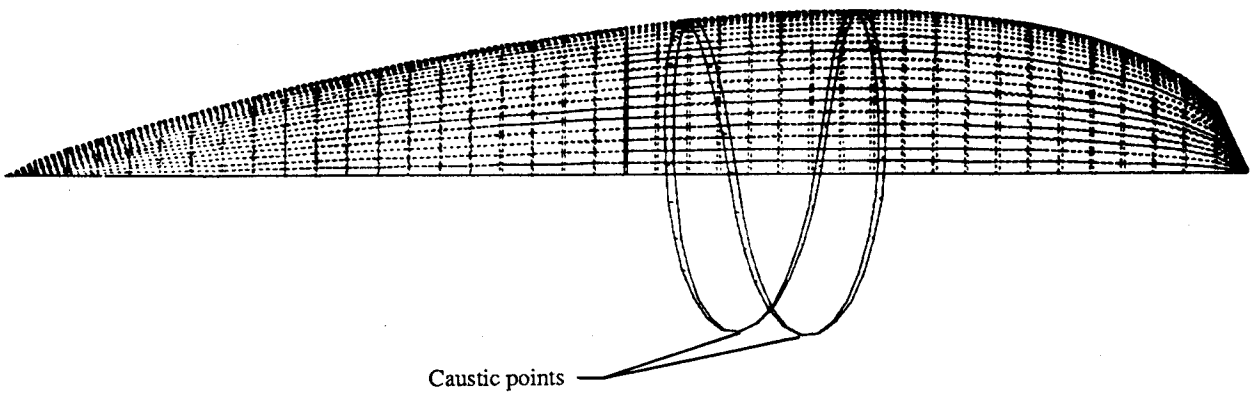

(b) Side view with only top half of surface displayed.

Figure 9. Closed-surface ray strip path corresponding to resonance condition.

this problem is the direct geodesic distance between the antennas.

As was mentioned, several papers by Überall and his associates (refs. 12 and 13) have discussed the relationship between surface wave frequencies and the normal modes of an elastic body, and calculations were performed for some separable surfaces. With the present capability to determine ray paths on a broad class of nonseparable surfaces, the potential exists for a variety of applications relating to elastic phenomena. Consider, for example, Lamb waves in a thin shell structure (with the usual restriction that the radii of curvature are large relative to the wave length, so that the wave speed is essentially constant for a given frequency). Then, in addition to the usual modes associated with ray paths along the maximum and minimum meridian lines, the possibility exists for a weaker kind of resonance associated with closed ray paths such as that shown in figure 9.

7. Concluding Remarks

A theory has been presented for computing surface waves and waves radiated from a smooth surface. With the assumption that attenuation of the surface wave is due only to radiation, the radiation coefficient was derived in terms of the attenuation factor. Then the excitation coefficient was determined by the reciprocity condition. Formulas for the shapes and the spreading of the radiated waves were derived, and some sample calculations were given. An investigation of resonant phase matching for nonseparable surfaces was presented with a sample calculation. Also included was a discussion of how such calculations might be related to resonant frequencies of nonseparable thin shell structures. A description was given of nonseparable surfaces that can be modeled in the vector form that facilitates use of the appropriate formulas of differential geometry.

NASA Langley Research Center
Hampton, VA 23665-5225
February 20, 1992

8. References

1. Keller, Joseph B.: A Geometrical Theory of Diffraction. *Calculus of Variations and Its Applications*, Lawrence M. Graves, ed., Volume III of *Proceedings of Symposia in Applied Mathematics,* McGraw-Hill Book Co., Inc., 1958, pp. 27–52.

2. Levy, Bertram R.; and Keller, Joseph B.: Diffraction by a Smooth Object. *Comm. Pure & and Appl. Math.,* vol. XII, no. 1, Feb. 1959, pp. 159–209.

3. Keller, Joseph B.; and Karal, Frank C., Jr.: Surface Wave Excitation and Propagation. *J. Appl. Phys.*, vol. 31, no. 6, June 1960, pp. 1039–1046.

4. Barger, Raymond L.: *A Procedure for Computing Surface Wave Trajectories on an Inhomogeneous Surface.* NASA TP-2929, 1989.

5. Überall, H.; Dragonette, L. R.; and Flax, L.: Relation Between Creeping Waves and Normal Modes of Vibration of a Curved Body. *J. Acoust. Soc. America*, vol. 61, no. 3, Mar. 1977, pp. 711–715.

6. Barger, Raymond L.; and Adams, Mary S.: *Semianalytic Modeling of Aerodynamic Shapes.* NASA TP-2413, 1985.

7. Pathak, Prabhakar H.; Burnside, Walter D.; and Marhefka, Ronald J.: A Uniform GTD Analysis of the Diffraction of Electromagnetic Waves by a Smooth Convex Surface. *IEEE Trans. Antennas & Propag.,* vol. AP-28, no. 5, Sept. 1980, pp. 631–642.

8. Überall, H.: Surface Waves in Acoustics. *Physical Acoustics—Principles and Methods,* Volume X, Warren P. Mason and R. N. Thurston, eds., Academic Press, Inc., 1973, pp. 1–59.

9. Grimshaw, R.: Propagation of Surface Waves at High Frequencies. *J. Inst. Math. & Its Appl.*, vol. 4, no. 2, June 1968, pp. 174–193.

10. Keller, Joseph B.; and Karal, Frank C., Jr.: Geometrical Theory of Elastic Surface-Wave Excitation and Propagation. *J. Acoust. Soc. America*, vol. 36, no. 1, Jan. 1964, pp. 32–40.

11. Struik, Dirk J.: *Differential Geometry.* Addison-Wesley Publ. Co., Inc., c.1950.

12. Flax, L.; Dragonette, L. R.; and Überall, H.: Theory of Elastic Resonance Excitation by Sound Scattering. *J. Acoust. Soc. America*, vol. 63, no. 3, Mar. 1978, pp. 723–731.

13. Merchant, Barbara L.; Nagl, A.; Stoyanov, Y. J.; Überall, H.; Brown, S. H.; and Dickey, J. W.: Resonant Phase Matching of Surface Waves on Impenetrable Spheroids. *J. Acoust. Soc. America*, vol. 80, no. 6, Dec. 1986, pp. 1754–1756.

REPORT DOCUMENTATION PAGE

Form Approved
OMB No. 0704-0188

1. AGENCY USE ONLY *(Leave blank)*	2. REPORT DATE	3. REPORT TYPE AND DATES COVERED
	March 1992	Technical Paper

4. TITLE AND SUBTITLE
Diffracted and Head Waves Associated With Waves on Nonseparable Surfaces

5. FUNDING NUMBERS
WU 505-59-53-01

6. AUTHOR(S)
Raymond L. Barger

7. PERFORMING ORGANIZATION NAME(S) AND ADDRESS(ES)
NASA Langley Research Center
Hampton, VA 23665-5225

8. PERFORMING ORGANIZATION REPORT NUMBER
L-16968

9. SPONSORING/MONITORING AGENCY NAME(S) AND ADDRESS(ES)
National Aeronautics and Space Administration
Washington, DC 20546-0001

10. SPONSORING/MONITORING AGENCY REPORT NUMBER
NASA TP-3169

11. SUPPLEMENTARY NOTES

12a. DISTRIBUTION/AVAILABILITY STATEMENT
Unclassified–Unlimited

Subject Category 02

12b. DISTRIBUTION CODE

13. ABSTRACT *(Maximum 200 words)*

A theory is presented for computing waves radiated from waves on a smooth surface. With the assumption that attenuation of the surface wave is due only to radiation and not to dissipation in the surface material, the radiation coefficient is derived in terms of the attenuation factor. The excitation coefficient is determined by the reciprocity condition. Formulas for the shape and the spreading of the radiated wave are derived, and some sample calculations are presented. An investigation of resonant phase matching for nonseparable surfaces is presented with a sample calculation. A discussion of how such calculations might be related to resonant frequencies of nonseparable thin shell structures is included. A description is given of nonseparable surfaces that can be modeled in the vector form that facilitates use of the appropriate formulas of differential geometry.

14. SUBJECT TERMS
Diffraction; Head waves; Nonseparable surfaces; Thin shell resonance

15. NUMBER OF PAGES
15

16. PRICE CODE
A03

17. SECURITY CLASSIFICATION OF REPORT	18. SECURITY CLASSIFICATION OF THIS PAGE	19. SECURITY CLASSIFICATION OF ABSTRACT	20. LIMITATION OF ABSTRACT
Unclassified	Unclassified		